Mon. Not. R. Astron. Soc. **339,** 913–924 (2003)

The discovery of two distant, massive clusters of galaxies in the *ROSAT* All-Sky Survey

A. C. Edge,[1⋆] H. Ebeling,[2†] M. Bremer,[3] H. Röttgering,[4] M. P. van Haarlem,[5] R. Rengelink[4] and N. J. D. Courtney[1]

[1]*Department of Physics, University of Durham, Durham DH1 3LE*
[2]*Institute for Astronomy, University of Hawaii, 2680 Woodlawn Drive, Honolulu, HI 96822, USA*
[3]*Department of Physics, Bristol University, Bristol BS8 1TL*
[4]*Leiden Observatory, Postbus 9513, 2300 RA Leiden, the Netherlands*
[5]*ASTRON, PO Box 2, 7990 AA Dwingeloo, the Netherlands*

Accepted 2002 November 6. Received 2002 July 5; in original form 2001 December 3

ABSTRACT

We discuss the radio, optical, and X-ray properties of two newly discovered, very X-ray luminous, distant clusters of galaxies. Both systems were noted as cluster candidates in a cross-correlation of data from the WENSS radio survey and the *ROSAT* All-Sky Survey. Follow-up observations performed by us and the Massive Cluster Survey (MACS) team confirmed both sources as distant galaxy clusters. The first cluster, MACS J0717.5+3745 at a redshift of $z = 0.5548$, contains a very extended, steep-spectrum radio source offset from the cluster core, making it the most distant radio relic known. The second cluster, MACS J1621.3+3810 at $z = 0.465$, is a strong cooling flow with a relatively weak central radio source. We present results from *ROSAT* High-Resolution Imager (HRI) observations of both clusters as well as from optical imaging and VLA radio interferometry observations. Our discoveries demonstrate that distant clusters can be efficiently identified in a relatively shallow X-ray survey, that radio/X-ray selection is efficient, and that both cooling flow and non-cooling flow clusters are selected.

Key words: galaxies: clusters: individual: MACS J0717.5+3745 – galaxies: clusters: individual: MACS J1621.3+3810 – cooling flows – radio continuum: galaxies.

1 INTRODUCTION

Clusters of galaxies host many of the most unusual radio sources known (e.g. Virgo-A; Cygnus-A; Perseus-A). The interaction of the relativistic plasma ejected from cluster members and the hot intracluster medium results in many complex radio structures (Böhringer et al. 1993; Carilli, Perley & Harris 1994; McNamara et al. 2000). Amongst the most complex of these radio structures are radio haloes and relics which are believed to occur during cluster–cluster mergers (Edge, Stewart & Fabian 1992; Tribble 1993). These radio haloes have relatively steep radio spectra ($\alpha = -1.0$ to -2.5) and hence are most prominent at low radio frequencies. Most published radio halo and relic sources lie in previously well-studied Abell clusters (Coma, Giovannini et al. 1993; A2256, Röttgering et al. 1994; A3667, Röttgering et al. 1997; Govoni et al. 2001) with only 1E 0657–56 (Liang et al. 2000) and Cl 0016+16 (Giovanni & Feretti 2000) known to lie in non-Abell clusters.

The correlation found by Liang et al. (2000) that the most powerful radio haloes are found in the most X-ray luminous clusters draws one to conclude that any search for radio haloes in distant clusters will also tend to find them in X-ray luminous clusters. Also, a study of radio sources in the X-ray flux-limited sample of Abell clusters (XBACs Ebeling et al. 1996) by Giovannini, Tordi & Feretti (1999) shows a higher detection rate of radio halo and relic sources in the more X-ray luminous clusters. Evidence linking these sources with cluster mergers is also found in the X-ray structural properties of clusters with radio haloes by Buote (2001). The theoretical modelling of cluster mergers and radio halo/relic formation has advanced greatly over the past decade (Tribble 1993; Röttiger et al. 1997; Röttiger et al. 1999; Ensslin & Bruggen 2001). These simulations demonstrate that both halo and relic phenomena are transient and have characteristic time-scales of the order of 10^9 yr or less.

The characteristic steep radio spectra of halo and relic sources makes selection at the lowest possible frequency the most efficient. The completion of the Westerbork Northern Sky Survey, WENSS (Rengelink et al. 1997) covering the sky north of a declination of 29° at 365 MHz presents a new opportunity to select haloes and relics. A search for haloes in all Abell clusters covered by WENSS has been performed by Kempner & Sarazin (2000) finding 18 sources of which 7 were previously unknown. The majority of the sources

⋆E-mail: Alastair.Edge@durham.ac.uk
†Guest Observer at the W.M. Keck Observatory.

in the Kempner & Sarazin (2000) sample are in X-ray luminous clusters ($L_x > 5 \times 10^{44}$ erg s^{-1}).

This paper presents the results of a joint radio/X-ray search for distant radio halo and relic sources in massive clusters of galaxies using data from both the WENSS and the *ROSAT* All-Sky Survey Bright Source Catalogue, RASS-BSC (Voges et al. 1999). This approach should favour the discovery of distant, X-ray luminous clusters which have not yet been identified and allow the evolution of radio halo and relic sources to be traced out to redshifts beyond 0.5. We first review the strategy used to select distant cluster candidates and its success rate. We then present a comprehensive analysis of the X-ray/optical/radio data for the two distant clusters discovered. Our paper concludes with a discussion of our findings in the larger context of ongoing, systematic searches for distant clusters of galaxies over a range of eight decades in wavelength.

We use $H_0 = 50$ km s^{-1} Mpc^{-1} and $q_0 = 0.5$ throughout this paper.

2 SOURCE SELECTION

The initial cluster candidate selection uses a cross-correlation of WENSS and RASS-BSC catalogues to find radio halo sources in distant clusters. Taking all unique WENSS radio sources away from the Galactic Plane ($|b| > 15^\circ$) with integrated flux densities brighter than 30 mJy within 60 arcsec of an X-ray source listed in the RASS Bright Source Catalogue (BSC, Voges et al. 1999) results in a total sample of 553 sources. The RASS-BSC coverage is essentially complete over the whole WENSS survey region (Dec $> 29^\circ$) with less than 3 per cent of the region with an exposure less than 240 s where the BSC count rate limit of 0.05 count s^{-1} would be less than 12 counts. Table 1 shows the relative numbers of these 553 sources with spectral indices greater than -0.5 or that that show a radio polarization of >2 per cent in the NVSS (where the flux density is above 40 mJy) for objects catalogued as active galactic nuclei (AGN), quasi-stellar objects (QSOs) or BLLacs, known Abell or BCS with $z < 0.3$ (Ebeling et al. 1998, 2000) clusters, clear random coincidences, for instance with an X-ray bright star and as yet unidentified sources that could conceivably be clusters. From the number of WENSS sources found at 5–15 arcmin from each of these object classifications we can estimate the number that would be expected by chance within 1 arcmin of the X-ray position which in all cases, apart from stars, this number is small.

Of the 97 sources that could be cluster X-ray sources, 51 of them were observable during our optical imaging run (i.e. between RA of 16 and 8 hr, see Section 3.1). A list of all 97 sources together with their probable identifications is provided as Table 2. As a control sample we also list a subset of objects that we have eliminated from the candidate list, mostly AGN identified after our observations.

Moderately deep imaging observations (at least 600 s in the *R*-band filter) of our candidate clusters were obtained with the Isaac Newton Telescope (INT) on La Palma in 1996 September (see Section 3). Due to time constraints, only a representative subsample of 26 sources could be covered. The vast majority (20) of these were found to be X-ray bright radio galaxies or BLLacs identified in subsequently published catalogues (e.g. RBS, Schwope et al. 2000), or relatively nearby ($z < 0.25$) clusters. Similarly, the majority of the sources not imaged by us with the INT are consistent with an isolated radio galaxy or a radio-loud AGN being the X-ray source. Only two of the sources observed by us were identified with distant ($z > 0.4$) clusters, and only one (later confirmed as MACS J0717.5+3745) harbours a diffuse radio source. The other cluster (MACS J1621.3+3810) contains a weak radio source coincident with the brightest galaxy. The WENSS radio sources in all other clusters feature low radio flux densities and are associated with the central galaxy. One unobserved source of our initial 50 has subsequently been identified as a similarly distant cluster (MACS J1824.3+4309); again the relatively weak radio source is associated with the brightest galaxy.

The majority (64 per cent) of the non-cluster radio sources in our initial source list are either polarized (>2 per cent in NVSS) and/or feature a flat spectrum ($\alpha_{0.365-1.4} > -0.5$). Conversely, only five of the 85 radio sources associated with confirmed galaxy clusters feature spectral indices in excess of -0.5 or similar polarization. Based on the X-ray imaging data available for these sources and the fact that the majority of them (three of five) are classified as extended in the RASS-BSC, we conclude that the radio source does not contribute significantly to the X-ray emission in these 'flat-spectrum' cluster sources. Of the cluster candidates, only three clusters (4C+55.16, 1RXS J103035.2+513229 and 1RXS J161415.1+544246) contain flat spectrum sources. The radio brightest of these (4C+55.16) has *ROSAT* and *Chandra* observations that confirm that the cluster is the dominant X-ray emitter (Iwasawa et al. 1999, 2001); the most distant (1RXS J103035.2+513229, $z = 0.518$ Caccianiga et al. 2000) has strong [O II] and is likely to be a strong cooling flow (not an active galaxy as Caccianiga et al. suggest); the third was covered in our INT imaging (see Table 1). While our strategy of excluding polarized and flat-spectrum sources does overlook some clusters, it does recover the vast majority.

The offsets between WENSS and RASS-BSC positions are consistent with the positional accuracy of the two surveys (<25 arcsec) in 85 per cent of the cases of the non-cluster sources. Fig. 1 shows a histogram of the number of sources in 30-arcsec bins for RASS-BSC sources coincident with WENSS sources within 15 arcmin, split on whether the X-ray source is a known or probable AGN (of any class), cluster or star. This figure shows the close association of AGN and the clear lack of association of stars with WENSS sources. The vast majority of the apparent AGN associations

Table 1. Relative numbers of *RASS-BSC/WENSS* coincidences within 60 arcsec split by radio properties and X-ray source identification.

	Flat ($\alpha_{365\,\mathrm{MHz}}^{1.4\,\mathrm{GHz}} > -0.4$)	Polarized ($P_{1.4} > 2$ per cent)	Flat and polarized	Neither	Number expected by chance
Confirmed AGN	66	75	44	102	9
Clusters ($z < 0.3$)	4	1	0	74	4
Clusters ($z > 0.3$)	0	0	0	6	0
Coincident stars	0	2	0	14	16
Other	32	26	10	97	6

Table 2. Identifications of cluster candidates and known clusters with $z > 0.3$. Sources marked with an asterisk do not meet the final selection criteria but were imaged to provide a control sample. References are given to all redshifts published in the last decade.

RASS-BSC source	WENSS source	offset (arcsec)	WENSS flux	Spectral Index	$P_{1.4}$ >2 per cent?	Obs?	Identification (reference)
J001827.8+294730*	WNB0015.8+2930	6.3	75	−0.58	N	Y	RBS 42, BLLac, $z = 0.100$ (1)
J002433.0+331237	WNB0021.9+3255	11.5	72	−1.12	N	N	MACS J0024.5+3312, cluster, $z = 0.226$ (2)
J002811.6+310342*	WNB0025.5+3046	15.3	611	−0.79	Y	Y	RGB J0028+310, Seyfert 1, $z = 0.500$ (3)
J003121.2+301558*	WNB0028.7+2959	11.0	306	−0.57	N	Y	$m_R = 16.3$, Seyfert 1, $z = 0.200$ (2)
J011513.2+405743	WNB0112.3+4041	39.2	32	−1.20	N	N	MACS J0115.2+4057, cluster, $z = 0.0978$ (4)
J012028.0+384918	WNB0117.6+3833	40.2	38	−2.02	N	N	MACS J0120.6+3849, cluster, z < 0.1 (5)
J020702.5+293035*	WNB0204.1+2916	32.8	7147	−1.11	N	Y	3C59, Seyfert 1, $z = 0.1096$
J031024.3+391109	WNB0307.1+3859	13.4	107	−0.71	N	N	$\|b\| < 20$, blue star, prob QSO
J053049.8+680304	WNB0525.4+6800	41.0	37	−0.72	N	Y	$\|b\| < 20$, cluster, z < 0.3 (5)
J062452.4+505353	WNB0620.9+5056	54.2	99	−0.78	N	Y	$\|b\| < 20$, cluster, z < 0.1 (5)
J062910.4+460637	WNB0625.4+4609	54.0	55	−1.07	N	N	$\|b\| < 20$, CIZA J0629.1+4606, cluster, $z < 0.15$ (5)
J063100.9+513314	WNB0627.1+5135	24.8	115	−1.14	N	N	$\|b\| < 20$, cluster, z < 0.1 (5)
J071148.0+321902	WNB0708.5+3223	41.3	284	−1.09	N	N	$\|b\| < 20$, CIZA J0711.7+3219, cluster, $z = 0.0672$ (6)
J071733.8+374520	WNB0714.2+3750	37.7	1308	−1.40	N	Y	MACS J0717.5+3745, cluster, $z = 0.550$ (5)
J072353.9+650450*	WNB0719.1+6510	15.5	3395	−0.88	Y	Y	4C+65.08, radio galaxy, $z = 0.2184$
J072650.3+310207	WNB0723.6+3107	14.7	540	−1.21	N	N	MACS J0726.8+3102, cluster, $z < 0.2$ (5)
J074012.2+723051*	WNB0734.4+7237	13.9	796	−1.00	Y	Y	8C 0734+726, radio galaxy/QSO
J074142.1+444251	WNB0738.2+4450	48.3	172	−0.93	N	N	MACS J0741.7+4442, cluster, $z < 0.15$ (5)
J074929.4+745142	WNB0743.2+7459	2.5	88	−0.51	N	N	RGB J0749+748, blue star, $m_R = 17.6$, prob QSO
J075334.6+385728	WNB0750.1+3905	33.9	37	−1.20	N	N	Blue galaxy, probably unrelated to radio source
J080730.4+340104	WNB0804.3+3409	28.9	56	−1.09	N	–	MACS J0807.5+3401, cluster, $z < 0.2$ (5)
J081021.3+421657	WNB0806.9+4225	35.2	62	−1.26	N	–	MACS J0810.3+4216, cluster, $z = 0.0664$ (7)
J082556.0+401406	WNB0822.6+4023	39.9	72	−0.73	N	–	Faint object, prob QSO
J083454.3+553417*	WNB0831.0+5544	6.2	9184	−0.08	N	–	4C+55.16, cluster, $z = 0.242$
J085011.2+360421	WNB0847.0+3615	10.2	135	−0.90	N	–	Zw1953, cluster, $z = 0.3737$ (8)
J085459.3+302120	WNB0851.9+3032	21.3	237	−1.42	N	–	Galaxy cluster, $z < 0.25$ (5)
J085610.0+541826	WNB0852.4+5430	33.5	173	−0.80	N	–	MACS J0856.1+5418, cluster, $z = 0.2539$ (9)
J090415.8+725947	WNB0859.1+7311	2.6	97	−1.42	N	–	Galaxy cluster, $z < 0.25$ (5)
J091346.0+405620	WNB0910.5+4108	14.8	54	−0.87	N	–	MACS J0913.7+4056, cluster/QSO2, $z = 0.442$
J091712.0+753043	WNB0911.6+7543	20.7	80	−0.75	N	–	Faint blue star, prob QSO
J092023.4+614717	WNB0916.4+6159	17.9	124	−1.22	N	–	Faint blue star, prob QSO
J094713.2+762317	WNB0942.0+7637	5.6	91	−1.04	N	–	MACS J0947.2+7623, RBS797, cluster, $z = 0.354$ (1)
J095013.5+290126	WNB0947.3+2914	57.2	48	−1.09	N	–	Galaxy cluster, z < 0.2 (5)
J100444.2+375156	WNB1001.7+3806	20.8	113	−1.09	N	–	faint blue galaxy, prob BLLac
J101738.5+593429	WNB1014.1+5949	31.6	43	−0.82	N	–	A959, cluster, $z = 0.353$
J103035.2+513229	WNB1027.4+5147	1.4	331	−0.43	N	–	Galaxy cluster, $z = 0.518$ (10)
J113313.3+500837	WNB1130.4+5025	1.9	2626	−0.84	N	–	MACS J1133.2+5008, cluster, $z = 0.389$ (5)
J113527.2+315337	WNB1132.8+3210	5.7	365	−1.29	N	–	MACS J1135.4+3153, cluster, $z = 0.231$ (11)
J114224.6+583151	WNB1139.6+5848	14.7	496	−0.88	N	–	MACS J1142.4+5831, A1351, cluster, $z = 0.322$
J114802.7+511611	WNB1145.3+5133	20.1	148	−1.46	N	–	Galaxy cluster, z < 0.3 (5)

Table 2 – *continued*

RASS-BSC source	WENSS source	offset (arcsec)	WENSS flux	Spectral Index	$P_{1.4}$ >2 per cent?	Obs?	Identification (reference)
J121508.8+462731	WNB1212.6+4643	20.9	612	−0.61	N	–	RGB J1215+467B, blue star, $m_R = 16.3$, prob QSO
J121614.1+524255	WNB1213.7+5259	26.2	60	−0.95	N	–	Blue galaxy, $m_R = 16.5$, prob BLLac
J121643.5+493855	WNB1214.2+4955	26.9	44	−1.03	N	–	Galaxy cluster, z < 0.25 (5)
J123658.8+631111	WNB1234.7+6327	11.7	74	−1.04	N	–	MACS J1236.9+6311, A1576, cluster, $z = 0.302$
J123819.4+412424	WNB1235.9+4140	18.7	110	−0.64	N	–	Faint blue star, FR II in *First*, prob QSO
J124608.0+705753	WNB1244.1+7114	14.4	140	−1.14	N	–	MS 1244.2+7114, cluster, $z = 0.225$
J125530.4+352126	WNB1253.1+3537	21.6	99	−0.64	N	–	MACS J1255.5+3521, cluster, $z = 0.1613$ (12)
J125908.1+412946	WNB1256.8+4145	32.4	207	−0.79	N	–	Galaxy cluster, $z < 0.25$ (5)
J130531.7+385523	WNB1303.2+3911	10.3	125	−0.79	N	–	faint galaxy, prob BLLac
J130610.4+514423	WNB1304.0+5200	15.7	159	−0.85	N	–	Galaxy cluster, $z < 0.3$ (5)
J132249.6+313844	WNB1320.4+3155	41.7	77	−0.99	N	–	MACS J1322.8+3138, cluster, $z = 0.3083$ (13)
J132543.9+413913	WNB1323.5+4154	30.6	54	−1.20	N	–	Galaxy cluster, $z < 0.2$ (5)
J133236.5+541855	WNB1330.6+5434	3.9	38	−0.81	N	–	NORAS, galaxy cluster, z = 0.101 (13)
J134503.8+404746	WNB1342.9+4102	10.9	38	−0.94	N	–	MACS J1345.0+4047, cluster, $z < 0.25$ (5)
J135441.3+771505	WNB1354.3+7730	56.5	165	−0.83	N	–	MACS J1354.6+7715, cluster, $z = 0.396$ (13)
J135916.0+744701	WNB1358.7+7501	13.4	214	−2.16	N	–	MACS J1359.2+7447, cluster, $z < 0.25$ (5)
J141141.1+340428	WNB1409.5+3418	9.4	197	−0.77	N	–	Faint galaxy, prob BLLac
J141121.2+521250	WNB1409.5+5226	40.6	61647	−0.74	N	–	MACS J1411.3+5212, 3C295, cluster, $z = 0.4605$
J141802.6+800710	WNB1419.1+8020	9.9	108	−0.70	N	–	NPM1G +80.0104, galaxy group, $z = 0.0461$ (14)
J142421.3+370554	WNB1422.2+3719	2.4	206	−0.71	N	–	Faint galaxy, prob BLLac
J144005.4+370747	WNB1438.0+3720	25.4	219	−1.97	N	–	MACS J1440.0+3707, cluster, $z = 0.097$ (11)
J144811.4+352708	WNB1446.1+3539	36.0	62	−0.75	N	–	Faint galaxy, prob BLLac
J145255.5+580251	WNB1451.6+5815	38.7	34	−1.11	N	–	MACS J1452.9+5802, A1995, cluster, $z = 0.316$
J150325.6+475828	WNB1501.7+4810	7.7	285	−0.74	N	–	Faint galaxy, prob BLLac
J151540.6+351037	WNB1513.7+3521	9.2	63	−0.75	N	–	Prob BLLac in cluster, point source in HRI
J152534.9+394649	WNB1523.6+3957	51.8	36	−0.53	N	–	Blue star, $m_R = 17.2$, prob AGN unrelated to radio
J153210.0+585434	WNB1531.0+5904	16.7	63	−0.53	N	-	Galaxy cluster, $z < 0.1$ (5)
J153253.7+302103	WNB1530.8+3030	55.5	116	−0.65	N	–	MACS J1532.8+3021, cluster, $z = 0.362$ (8)
J153520.8+342251	WNB1533.4+3433	40.1	674	−0.98	N	–	MACS J1535.3+3422, cluster, $z = 0.235$ (4)
J155418.3+464400	WNB1552.7+4652	41.0	57	−0.57	N	–	Blue star, $m_R = 17.6$, FR II in *First*, prob QSO
J160517.3+375655	WNB1603.4+3804	25.4	305	−0.69	N	N	blue star, $m_R = 16.6$, unrelated to radio source
J161035.0+480017	WNB1609.1+4808	47.2	97	−0.52	N	Y	blue galaxy counterpart, $m_R = 17.8$
J161415.1+544246*	WNB1613.0+5450	28.9	39	−0.43	N	Y	galaxy cluster, $z = 0.331$ (5)
J162124.0+381002	WNB1619.6+3817	10.9	43	−1.14	N	Y	MACS J1621.4+3810, cluster, $z = 0.465$ (5)
J162724.3+424041	WNB1625.7+4248	54.3	78	−0.99	N	N	NGC 6159, galaxy group, $z = 0.0315$
J163726.2+454746	WNB1635.9+4553	26.4	94	−0.54	N	N	RGB J1637+457, galaxy, $m_R = 16.3$, prob BLLac
J163856.0+433507*	WNB1637.3+4340	5.1	718	−0.98	Y	Y	galaxy counterpart, $m_R = 18.6$
J164843.5+800506	WNB1652.5+8009	56.7	80	−0.92	N	N	galaxy cluster, $z < 0.25$ (5)
J165358.1+441042	WNB1652.3+4415	36.9	82	−0.58	N	N	MACS J1653.9+4410, cluster, $z = 0.115$ (4)
J170425.2+333145*	WNB1702.5+3335	14.5	105	−0.51	Y	Y	Broad Line Radio Galaxy, $z = 0.280$ (5)

Table 2 – *continued*

RASS-BSC source	WENSS source	offset (arcsec)	WENSS flux	Spectral Index	$P_{1.4}$ >2 per cent?	Obs?	Identification (reference)
J171304.5+352335*	WNB1711.3+3526	33.9	58	−1.17	N	Y	RBS 1631, Seyfert 1, $z = 0.0850$ (8)
J171322.8+325631*	WNB1711.4+3259	40.2	293	−0.87	Y	Y	RGB J1713+329, BLRG, $z = 0.1010$ (15)
J172015.5+353622	WNB1718.4+3538	20.8	103	−0.93	N	Y	MACS J1720.2+3536, Zw8201, cluster, $z = 0.3913$ (4)
J172205.0+565450	WNB1721.2+5657	9.0	108	−0.68	N	N	Blue star, prob QSO
J172635.0+392321	WNB1724.8+3926	56.3	45	−0.56	N	N	MACS J1726.5+3923, cluster, $z = 0.125$ (4)
J173354.5+300026	WNB1731.9+3002	11.3	392	−0.79	N	N	galaxy cluster, $z < 0.15$ (5)
J174248.6+390027	WNB1741.1+3901	31.5	1648	−1.20	N	N	RXJC 1742.8+3900, cluster, $z = 0.0423$ (9)
J174537.3+395128*	WNB1743.9+3952	5.8	2050	−0.87	N	N	BLLac in cluster, $z = 0.267$ (15)
J174815.7+494156	WNB1747.0+4942	10.6	251	−0.75	N	N	MACS J1748.2+4941, cluster, $z = 0.188$ (4)
J175004.4+470037	WNB1748.4+4701	37.5	304	−0.83	N	Y	MACS J1750.0+4700, cluster, $z = 0.160$ (9)
J175131.2+471315*	WNB1750.7+4714	31.7	170	−0.60	N	Y	RGB J1751+472, QSO, $z = 1.480$ (15)
J175441.5+345937	WNB1752.9+3500	33.9	69	−1.01	N	Y	MACS J1754.6+3459, cluster, $z = 0.254$ (4)
J175951.3+454346*	WNB1758.4+4544	50.3	412	−0.65	Y	Y	faint blue star, confirmed with HRI, $m_R = 18.8$
J180242.4+424734	WNB1801.1+4247	33.9	78	−1.17	N	N	RXJC 1802.7+4247, cluster, $z = 0.0499$ (11)
J181746.1+682424	WNB1817.9+6823	11.0	57	−1.03	N	Y	MACS J1817.7+6824, cluster, $z = 0.295$ (4)
J182310.7+332420	WNB1821.3+3322	18.5	766	−1.06	N	N	MACS J1823.1+3324, cluster, $z = 0.1080$ (9)
J182407.7+302933	WNB1822.2+3027	12.1	64	−1.00	N	N	$\|b\| < 20$, CIZA J1824.1+3029, cluster, $z < 0.1$ (5)
J182418.7+430954	WNB1822.7+4308	4.5	73	−0.58	N	N	MACS J1824.3+4309, cluster, $z = 0.487$ (4)
J182903.8+691350	WNB1829.4+6911	17.6	207	−2.08	N	Y	MACS J1829.0+6913, cluster, $z = 0.203$ (4)
J183235.1+684805	WNB1832.8+6845	3.1	559	−0.98	N	Y	RGB J1832+688, cluster, $z = 0.205$ (16)
J184429.9+534847	WNB1843.4+5346	39.8	118	−0.90	N	N	Galaxy cluster, z < 0.15 (5)
J184828.3+750326	WNB1849.9+7459	3.6	130	−0.85	N	N	MACS J1848.4 + 7503, cluster, $z < 0.15$ (5)
J192413.2+665637	WNB1924.0+6650	5.1	71	−0.91	N	N	IRAS galaxy, $m_R = 14.4$, prob AGN
J193113.8+600001	WNB1930.4+5953	14.3	197	−0.66	N	N	$\|b\| < 20$, cluster, $z < 0.15$ (5)
J193818.5+540928	WNB1937.1+5402	23.3	47	−0.76	N	N	$\|b\| < 20$, CIZA J1938.3+5409, cluster, $z = 0.260$ (6)
J194017.2+680738	WNB1940.2+6800	7.5	384	−1.30	N	N	MACS J1940.2+6807, cluster, $z = 0.166$ (4)
J194423.1+655216	WNB1944.0+6545	8.9	1367	−1.69	N	N	$\|b\| < 20$, cluster, $z < 0.3$ (5)
J200307.6+682945	WNB2002.9+6820	23.3	120	−0.67	N	Y	$\|b\| < 20$, cluster, $z < 0.2$ (5)
J214613.5+850149	WNB2150.4+8447	6.1	84	−0.86	N	N	BLLac or cluster, $z < 0.25$ (5)
J215623.8+331829	WNB2154.2+3304	11.7	1035	−1.38	N	N	$\|b\| < 20$, cluster, $z = 0.0784$ (17)
J223758.3+410109	WNB2235.6+4045	55.0	342	−0.78	N	N	$\|b\| < 20$, cluster, $z < 0.15$ (5)
J231947.4+425117	WNB2317.4+4234	14.5	321	−0.78	N	N	NGC 7618, $\|b\| < 20$, galaxy group, $z = 0.0175$

References: (1) Fischer et al. (1998) (2) Wei et al. (1999) (3) Wei et al. (1998) (4) Ebeling, Edge & Henry, in preparation (5) this work (6) Ebeling et al. (2003) (7) Vikhlinin et al. (1998) (8) Crawford et al. (1999) (9) Bauer et al. (2000) (10) Caccianiga et al. (2000) (11) Brinkmann et al. (2000) (12) Huchra, Geller & Corwin (1995) (13) Böhringer et al. (2000) (14) Falco et al. (1999) (15) Laurent-Muehleisen et al. (1998) (16) Moran et al. (1996) (16) Ebeling et al. (2002) (17) Motch et al. (1998).

between 30 and 60 arcsec have significant radio structure that exaggerates the radio/X-ray offset. One significant exception to this is 1RXS J175951.3+454346, for which a follow-up *ROSAT* HRI observation reveals a point source that is coincident with the radio source but 50 arcsec from the RASS-BSC position. The significant source extent listed in the RASS-BSC for this source (55 arcsec, with a likelihood of 10) could be explained by a blend at the resolution of the RASS. However, no other source is detected by the

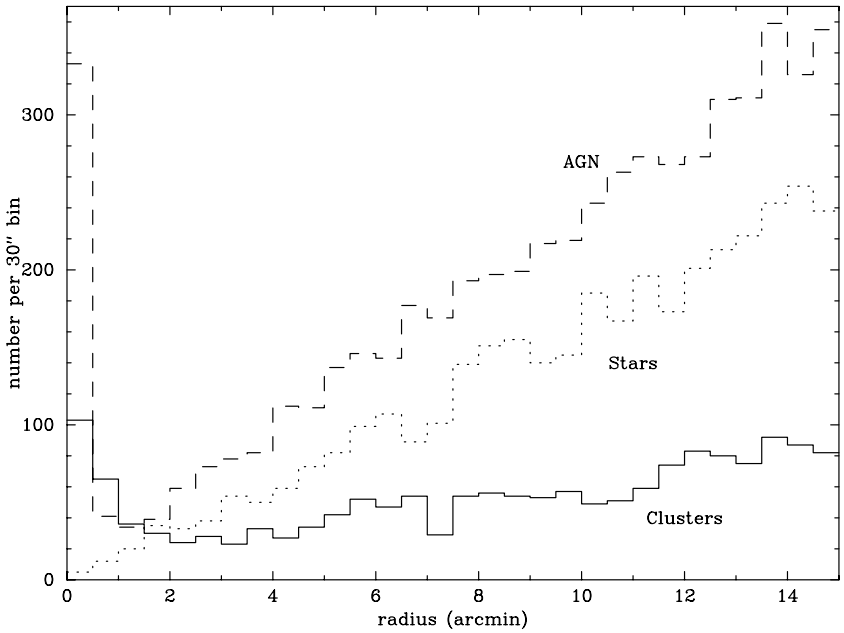

Figure 1. Histogram of the number of coincidences between WENSS and RASS-BSC sources divided into 30-arcsec bins for X-rays sources split into known or probable AGN of any type (dashed line), known or probable clusters (solid line), or stars (dotted line). Random associations appear as a linear trend with increasing radius (as shown by the stars) Note the strong excess of AGN within 30 arcsec and the broader distribution of clusters.

HRI within 10 arcmin and the total count rate is consistent with that expected given the RASS-BSC count rate making blend with a variable source unlikely. This offset is most probably a systematic shift introduced by the RASS analysis software.

The radio/X-ray offsets for galaxy clusters are larger on average with only 45 per cent within 25 arcsec. This reflects both the extended nature of the X-ray emission and the fact that many of the radio sources are associated with cluster galaxies outside the cluster centre.

The relatively high proportion of clusters at low Galactic latitude (almost half) in our study is the result of the preferential removal of Abell or BCS clusters at $|b| > 20^\circ$ which account for 70–80 per cent of the $z < 0.15$ clusters in RASS clusters samples to date. Many of the clusters found by us at $|b| < 20^\circ$ have also been discovered by the CIZA X-ray survey (Clusters In the Zone of Avoidance; Ebeling, Mullis & Tully 2002). A similar effect applies to identifications of non-cluster sources at lower Galactic latitudes as most systematic identification programmes have so far concentrated on higher latitudes.

Five of the six distant ($z > 0.4$) clusters identified with this hybrid radio/X-ray/optical selection technique were also independently recovered (together with many other similar clusters) by the Massive Cluster Survey (MACS, Ebeling, Edge & Henry 2001) which is based on the same X-ray source list (RASS-BSC) but requires only optical imaging to select distant cluster candidates. Two of these six clusters are well studied in the literature (IRAS 0910+41, Fabian et al. 2000 and 3C295, Allen et al. 2001). The only non-MACS cluster (1RXS J103035.2+513229), as mentioned above, is probably a flat-spectrum radio source in a strong cooling flow (although this needs optical imaging for confirmation) and is below the MACS flux limit. Redshifts for these WENSS-selected, distant clusters and other clusters at lower redshift were obtained as part of the MACS spectroscopic follow-up programme (see Section 3).

3 OPTICAL PROPERTIES

3.1 Observations

Following up on the initial INT images of J071733.8+374520 and J162625.5+351331 taken on 1996 September 18 and 19 in fair to good conditions, we obtained moderately deep optical images of both clusters in the *V*, *R*, and *I* passbands using the University of Hawaii's (UH) 2.2-m telescope in 2000 September and July, respectively. Three dithered exposures of 240 s duration were taken through each of the three filters. Standard image processing techniques were applied to subtract the detector bias level, flatten the raw images, and remove artefacts caused by cosmic rays and cosmetic flaws of the CCD. Colour representations of the processed images are shown in Fig. 2, with the *V*, *R*, and *I* images being used for the *B*, *G*, and *R* channels of the composite image.

A low-dispersion spectrum of the central galaxy in MACS J1621.3+3810 was obtained on 1999 August 11, with the Wide-Field Grism Spectrograph (WFGS) at the UH 2.2-m telescope. We used the standard Tektronix 2048 × 2048 CCD and a 400 l mm^{-1} grism (which yields a dispersion of 3.55 Å pixel^{-1} over a spectral range from 3000–10 000 Å), a 1.5 arcsec longslit, and an exposure time of 3 × 15 minutes. Multiple spectra of galaxies in MACS J0717.5+3745 were obtained with the Low-Resolution Imaging Spectrograph (LRIS, Oke et al. 1995) at the Keck 10-m telescope on 1998 October 25 and 2000 January 29. For our LRIS observations we used the standard SITE 2 k CCD with the 300/5000 grism and the GG495 highpass filter (which yields a dispersion of 2.28 Å pixel^{-1} and a spectral range from 5000 to approximately 9500 Å), a 1.5-arcsec long slit, and exposure times of 2 × 5 and 3 × 5 min for two long-slit orientations. Standard spectral data reduction procedures were applied to remove bias pixel-to-pixel variations in the CCD sensitivity as well as the signature of the spectrograph response function. The LRIS results are part of a larger multi-object

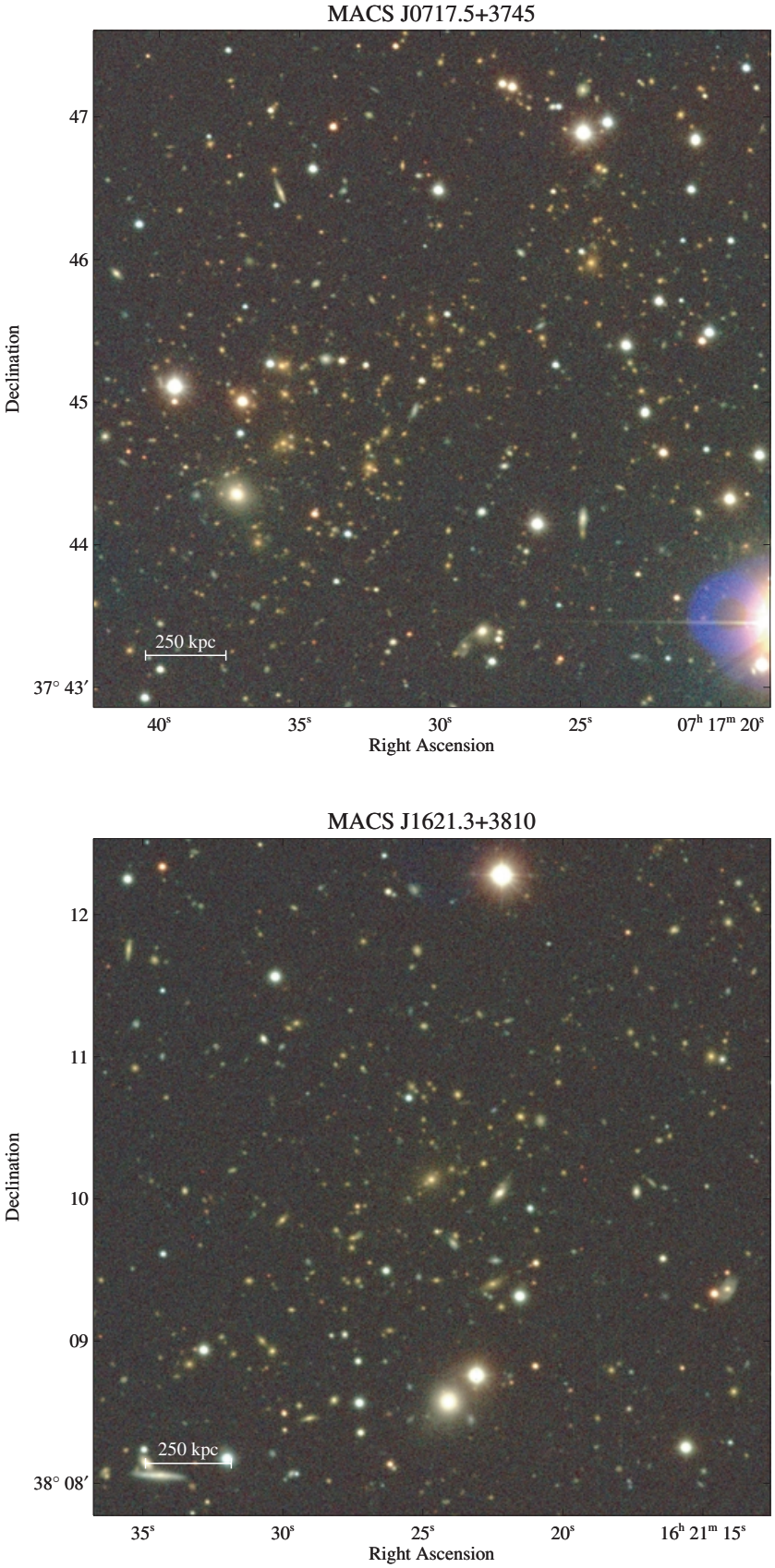

Figure 2. Colour images of the newly discovered distant clusters MACS J0717.5+3745 ($z = 0.548$) and MACS J1621.3+3810 ($z = 0.465$). Both images are based on data taken with the UH 2.2-m telescope in the V, R, and I passbands (3 × 240 s each), with I, R, and V mapped to the R, G, and B colour channels, respectively.

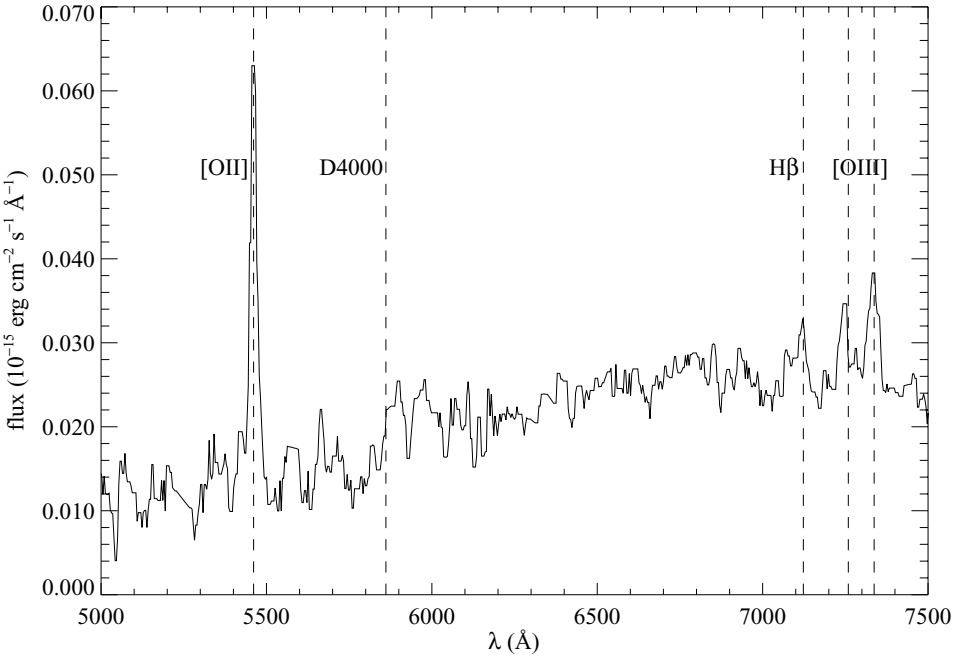

Figure 3. The UH 2.2-m WFGS spectrum of the central galaxy of MACS J1621.3+3810. The spectrum shows strong [O II] emission characteristic of a strong cooling flow. The spectrum has been median-averaged over 5 pixels in wavelength for presentation.

spectroscopic study of MACS clusters and will be presented in a later paper.

3.2 Results

The colour images of MACS J0717.5+3745 and MACS J1621.3+3810 (Fig. 2) show a remarkable difference in their optical morphology. Whereas MACS J1621.3+3810 is dominated by a central cD galaxy and exhibits little apparent subclustering, the much more extended system MACS J0717.5+3745 is characterized by a pronounced double structure and the total absence of a classical cluster core. The highly disturbed optical morphology of MACS J0717.5+3745 suggests that the system has recently been disrupted by the infall, and passage, of a sizeable subcluster. This tentative interpretation is supported by the presence of a diffuse radio relic (see Section 4.2) and by the unusual X-ray morphology of the system (see Section 5.2).

The WFGS spectrum of the central galaxy of MACS J1621.3+3810 (Fig. 3) shows strong [O II] emission indicating the presence of a strong cooling flow (Peres et al. 1998). This is supported by the X-ray imaging data (see Section 5.2).

4 RADIO PROPERTIES

4.1 Observations

The resolution of WENSS (Rengelink et al. 1997) and NVSS (Condon et al. 1998) images are insufficient to resolve the diffuse radio emission in MACS J0717.5+3745. We therefore also inspected higher-resolution images from the FIRST survey (Becker, White & Helfand 1995), and obtained additional radio images at 1.46 and 8.4 GHz using the Very Large Array (VLA) in its B- and C-array configuration respectively. The 1.4-GHz data were obtained on 1997 February 13 with an exposure of 580 s. Due to calibration problems and poor UV coverage the resulting imaging does not improve upon the FIRST survey data but does confirm the morphology in the regions of high radio surface brightness. The additional 8.4-GHz data were obtained on 1998 November 22 with an exposure of 480 s. We also obtained VLA data for MACS 1621.3+3810 at 1.46 and 8.4 GHz on 1997 August 3 in the CS-array configuration with exposures of 600 and 280 s respectively.

4.2 Results

As shown in Fig. 4, the FIRST image of MACS J0717.5+3745 shows a wealth of structure in the radio source which strongly resembles the complex radio relics seen in (for instance) A2256 (Röttgering et al. 1994) and A3667 (Röttgering et al. 1997). There are individual radio sources embedded in the more diffuse radio emission.

Our VLA images of MACS J0717.5+3745 indicate that there is no strong unresolved (<0.5 arcsec) source above 5 mJy at 8.4 GHz associated with any of the sub-components of the radio emission; hence it is unlikely that the X-ray emission is related to nuclear activity (as is confirmed by X-ray imaging). The bright foreground galaxy at $07^{\rm h}17^{\rm m}37\overset{\rm s}{.}2 + 37^{\circ}44'21''$ (J2000) is detected at 7.3 ± 0.4 mJy and 1.9 ± 0.2 mJy at 1.4 and 8.4 GHz respectively giving a spectral index of -0.77 ± 0.09.

The overall radio photometry of the source in MACS J0717.5+3745 is consistent with a spectral index of -1.3, a not particularly steep spectrum compared to that of other radio haloes and relics. This may be an indication that this source is relatively young and has not suffered significant spectral ageing.

For MACS J1621.3+3810 the radio data show that the WENSS source is coincident with the central dominant galaxy of the cluster with a 1.46-GHz flux density of 8.4 ± 1.3 mJy, consistent with the NVSS value of 9.3 mJy. Our VLA CS 1.4-GHz image shows no significant structure on scales of larger than 12 arcsec and the corresponding FIRST Survey source shows no evidence for extent above 2 arcsec (but with also a lower flux density 5.6 mJy). Our VLA 8.4-GHz image is not deep enough to set a firm limit on the

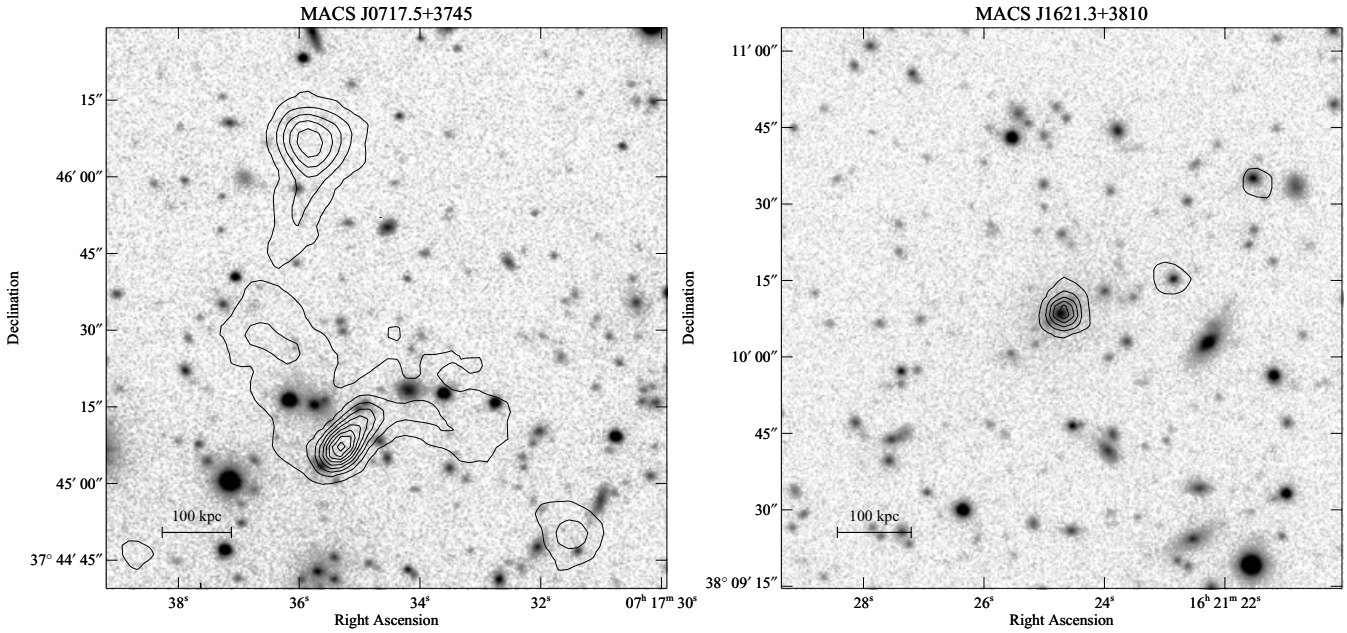

Figure 4. FIRST images of the radio emission in the cores of MACS J0717.5+3745 and MACS J1621.3+3810 overlaid on *R*-band images of the clusters obtained with the UH 2.2-m telescope. The contours are spaced by 1 mJy beam^{-1} with the lowest contour at 0.5 mJy beam^{-1}. The very extended radio emission observed near the core of MACS J0717.5+3745 is not obviously associated with any optical counterpart, whereas the point-like radio emission observed in MACS J1621.3+3810 originates clearly from the BCG.

extent of the emission and sets a weak limit of 1.1 ± 0.4 mJy on the flux density. The relatively compact nature of this source, its spectral index from 327 MHz to 8.4 GHz of −1.35 and its radio power of 4×10^{25} W Hz^{-1} are all consistent with features found in many other, lower redshift central cluster galaxies (Burns 1990; Ball et al. 1993).

The radio data for the other WENSS-selected clusters at lower redshifts yield spectral indices of the central galaxies ranging from −1.9 to −0.3 with the majority (60 per cent) between −1.1 and −0.7 which are again consistent with other X-ray selected central cluster galaxies.

5 X-RAY PROPERTIES

5.1 Observations

ROSAT HRI observations of MACS J0717.5+3745 and MACS J1621.3+3810 were awarded to us in AO-8; the effective on-axis exposure times are 19 467 and 30 675 s, respectively. Both HRI data sets were processed by us using the CAST˙HRI package, kindly made available by Steve Snowden and modified by us to use smaller (2.5×2.5 arcsec^2) pixels. The immediate data products generated by CAST˙HRI are images of the total observed counts, the projected particle background, and the effective exposure time (including vignetting and spatial variations in the detector sensitivity). Having eliminated point sources within the field of view, we flatten the raw image by subtracting the particle component of the background (which is not subject to vignetting) and then dividing by the exposure map. The resulting image is temporarily smoothed with a top-hat kernel of 1 arcmin in radius and the mean of the pixel values in the resulting image (excluding a region of radius 2 Mpc around the cluster as well as the field edges) is adopted as the cosmic background value. An improved value of the centre of the cluster emission is then determined as the position of the maximum of background-corrected signal on a scale of 250 kpc. In practice we compute this position as the brightest image pixel of the convolution of the raw X-ray image, with a Gaussian kernel of 250 kpc in standard deviation. Finally, the radial X-ray surface brightness profile is computed in circular annuli 2.5-arcsec wide; for each surface brightness value we propagate all errors, i.e. the uncertainties in the values of the particle and cosmic background as well as the Gaussian error in the number of detected photons.

For an assessment of the overall X-ray morphology of the source we use the 'ASMOOTH' algorithm of Ebeling, White & Rangarajan (2003) to adaptively smooth the observed emission. The smoothing kernel is a Gaussian scaled to ensure a minimal significance 3σ for all features in the smoothed image.

5.2 Results

Isointensity contours of the adaptively smoothed X-ray emission from each cluster overlaid on the optical cluster images are shown in Fig. 5. For both clusters the HRI observations confirm that the X-ray emission arises predominantly from extended diffuse gas, although the two clusters differ considerably in their X-ray morphology.

As shown in Fig. 5, the emission from MACS J0717.5+3745 is broadly extended with a mild peak embedded in a large region of relatively low X-ray surface brightness. Interestingly, the X-ray peak does not coincide with either of the two galaxy concentrations which characterize the optical appearance of the clusters (Fig. 2), but rather falls exactly between them. The pronounced asymmetry and the exceptional misalignment of the gas and galaxy distributions lend strong support to the notion that MACS J0717.5+3745 is undergoing a major merger (see also Section 3.2).

A deprojection analysis of the HRI X-ray data was performed assuming a cluster potential with a velocity dispersion of 1200 km s^{-1} and a core radius of 300 kpc, using the method outlined in

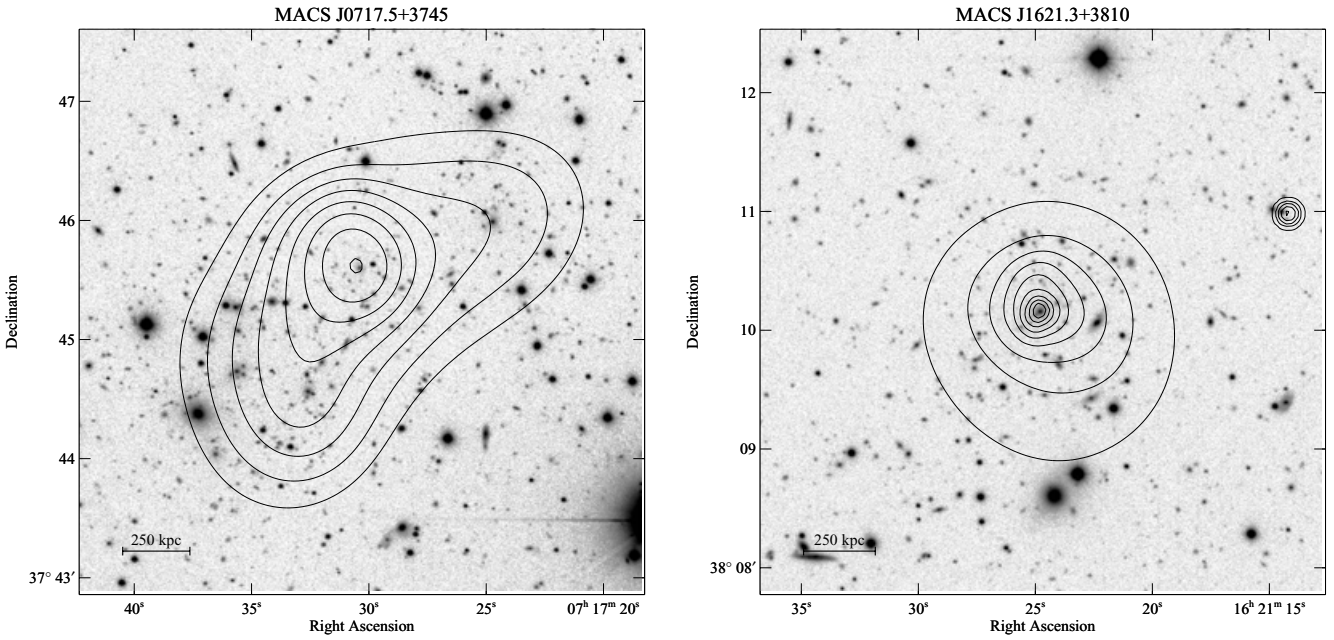

Figure 5. Isointensity contours of the adaptively smoothed X-ray emission from MACS J0717.5+3745 and MACS J1621.3+3810 (as observed with the *ROSAT* HRI) overlaid on *R*-band images of the clusters obtained with the UH 2.2-m telescope. Contours are logarithmically spaced with the lowest contour being a factor of 1.5 (1.3) above the background, and adjacent contour levels differing by 30 (50) per cent for MACS J0717.5+3745 (MACS J1621.3+3810). Note the very different X-ray morphology of these two clusters. The serendipitous point source toward the right edge of the right-hand image illustrates the diffuse nature of the cluster emission.

White, Jones & Forman (1997) where the input velocity dispersion is scaled to the X-ray luminosity of the cluster and the core radius is selected to return an isothermal temperature profile. This potential gives a temperature of 13 keV and implies an upper limit to the mass deposition rate for MACS J0717.5+3745 of 9 $M_\odot$ yr^{-1} and a central cooling time of $2.1 \pm 1.9 \times 10^{10}$ yr in the central bin of 74 kpc.

By way of contrast, the HRI image of MACS J1621.3+3810 shows a very pronounced peak at the location of the central cluster galaxy indicating the presence of a strong cooling flow. On a larger scale, the emission appears compact and spherically symmetric. The X-ray morphology of MACS J1621.3+3810 is thus in very good agreement with the relaxed appearance of the system in the optical waveband. The deprojection results for MACS J1621.3+3810 assuming a potential with a velocity dispersion of 1100 km s^{-1} and core radius of 130 kpc (which gives an approximately isothermal temperature profile of 11 keV) show a cluster with a mass deposition rate of 292 ± 63 $M_\odot$ yr^{-1} and a central cooling time of $1.6 \pm 0.3 \times 10^9$ yr in the central bin of 52 kpc.

We use the HRI data shown in Fig. 5 to measure total X-ray fluxes and luminosities for either cluster. Following the procedure described at the beginning of Section 5.1 we obtain improved celestial coordinates for the X-ray centroids of ($16^h21^m25\overset{s}{.}2$, $+38^\circ10'10\overset{''}{.}7$) (J2000) and ($07^h17^m30\overset{s}{.}1$, $+37^\circ45'37\overset{''}{.}2$) (J2000) for MACS J1621.3+3810 and MACS J0717.5+3745, respectively. The total cluster count rates within a circular aperture centred on these coordinates are (0.031 ± 0.002) s^{-1} (MACS J1621.3+3810, $r < 1$ Mpc) and (0.049 ± 0.004) s^{-1} (MACS J0717.5+3745, $r < 1.5$ Mpc). Adopting a spectrum appropriate for a hot, diffuse plasma (Raymond & Smith 1977) parametrized by a metallicity of 0.2 solar and a self-consistent gas-temperature estimated from the $L_X - kT$ relation of White et al. (1997), and absorbed by the Galactic equivalent column density of neutral hydrogen (Dickey & Lockman 1990) in the direction of either system, we convert the HRI count rates to total, unabsorbed X-ray fluxes in the 0.1–2.4 keV band of $(1.29 \pm 0.08) \times 10^{-12}$ erg cm^{-2} s^{-1} (MACS J1621.3+3810) and $(2.78 \pm 0.20) \times 10^{-12}$ erg cm^{-2} s^{-1} (MACS J0717.5+3745). At the appropriate cluster redshift, these fluxes correspond to rest-frame luminosities in the 0.1–2.4 keV band of $(1.14 \pm 0.07) \times 10^{45}$ erg s^{-1} (MACS J1621.3+3810) and $(3.29 \pm 0.24) \times 10^{45}$ erg s^{-1} (MACS J0717.5+3745), values that place both systems among the 10 most X-ray luminous clusters known at $z > 0.45$ (pre-MACS era). Note that the implied gas temperatures of 9.3 and 14.7 keV used here are consistent with the values assumed in the deprojection analysis described above and the measured fluxes are consistent with those from the RASS-BSC (1.25 ± 0.17 and $1.95 \pm 0.32 \times 10^{-12}$ erg cm^{-2} for MACS J1621.3+3810 and MACS J0717.5+3745) given the BSC analysis assumes a point source profile.

6 DISCUSSION

The discovery of two very X-ray luminous ($L_X > 1 \times 10^{45}$ erg s^{-1}, 0.1–2.4 keV), distant ($z > 0.45$) clusters from *ROSAT* All-Sky Survey data underlines the enormous potential of this shallow-but-wide survey for distant cluster studies. Clusters like MACS J0717.5+3745 and MACS J1621.3+3810 are not readily identifiable from optical plate material and require dedicated CCD imaging to be confirmed. However, thanks to the initial X-ray selection of cluster candidates these optical follow-up observations are significantly more efficient than generic optical searches for distant clusters, and the scientific return is high. Only two X-ray luminous clusters at $z > 0.5$ were known before the completion of the RASS, MS0015.9+1609 and MS0451.6−0305 (Gioia et al. 1990). The MACS sample currently contains both of these EMSS clusters, as well as MACS J0717.5+3745 and seven others.

The discovery of a radio relic in MACS J0717.5+3745 makes it the most distant example yet found (it is fractionally more distant than CL 0016+16) and is consistent with the observed trend for more luminous clusters to host more powerful radio haloes and relics (Liang et al. 2000).

In the light of statistics of more nearby clusters showing that between 10–20 per cent of X-ray luminous clusters host a radio halo or relic, the discovery of one relic in ten $z > 0.5$ clusters is not unexpected. Our discovery is more remarkable when one considers that MACS J0717.5+3745 is one of only 4 distant ($z > 0.5$) MACS clusters covered by the WENSS survey. If, on the other hand, the number of MACS clusters between redshifts of 0.3 and 0.5 in the WENSS survey (27) without a halo or relic is taken into account the frequency of radio relics is much lower.

The low number of detected radio haloes and relics in our study could, at least in part, be related to the relatively small maximal separation of 60 arcsec used in the cross-correlation between the radio and X-ray samples. For the majority of the $z > 0.3$ clusters detected in the RASS-BSC this corresponds to projected metric radii less than 1 Mpc, whereas many of the best known radio relics in more nearby clusters are at considerably large projected radii. However, extending the cross-correlation between X-ray and radio samples to larger angular separations would dramatically increase the number of random coincidences and would have produced a prohibitively large target list for optical imaging. This problem can be circumvented by using an X-ray sample consisting exclusively of distant clusters, i.e., MACS (Ebeling et al. 2001). Examining the 31 MACS clusters at $z > 0.3$ in the WENSS survey area to 10 arcmin, we find just one comparable radio halo or relic candidate in the *First*/NVSS images of the 41 WENSS sources within a projected radius of 1–10 arcmin (i.e. those not already covered in this study). The one candidate is MACS J1752.0+4440 ($z = 0.366$; Ebeling, Edge & Henry, private communication) with two moderately steep ($\alpha < -1.3$) sources 2 arcmin either side of the cluster centre. This cluster was not covered by FIRST and has not yet been observed by the VLA so this candidate remains unconfirmed. The results of this wider subsample imply that the WENSS sources at radii larger than 4 arcmin have a constant surface density (14 ± 3 deg $^{-2}$ - consistent with the overall WENSS surface density of 15.5 deg^{-2} at our flux density limit of 30 mJy) so are very likely to be background or foreground sources. Extrapolating this surface density to smaller radii indicates that an excess of 16–20 sources is present, of which 14 are within 1 arcmin. Nine of these sources are related to the central dominant galaxy, three are head–tail sources, one is a QSO in the cluster, and the final one is the relic in MACS J0717.5+3745. This implies that our use of a search radius of 1 arcmin was reasonable and recovers 70–85 per cent of the cluster-related sources at $z > 0.3$.

From this targeted cluster search, we conclude that radio haloes and relics are as rare at high redshift as they are at low redshift. This is apparently at odds to the conclusion drawn by Liang et al. (2000) using the Giovannini et al. (1999) data, although it ought to be noted that the radio flux and surface brightness limits reached are different. For the MACS clusters, the WENSS and NVSS surveys do not reach the same depth in terms of radio power achieved by the study of more nearby Abell clusters by Giovannini et al. (1999) using NVSS alone. Taking the radio power limit of 10^{25} W Hz^{-1} into account the Giovannini et al. (1999) survey would predict only two haloes/relics more powerful than this limit in the MACS sample of 31, so these two studies are consistent. Our strategy of observing coincident radio and X-ray sources was successful but not as efficient as a more focussed comparison of identified clusters with extended, steep spectrum radio sources. Repeating the Giovannini et al. (1999) analysis on the MACS cluster sample will require dedicated VLA imaging.

As illustrated above, the majority of our joint X-ray/radio selected clusters are cases where the central galaxy is the primary radio source. This illustrates the higher likelihood for the central galaxy to be a radio source (Burns 1990) and highlights the possible inclusion of clusters in BLLac searches. The latter point is demonstrated in Perlman et al. (1998) where the central galaxy in Abell 11 is selected in a X-ray/radio study to identify BLLacs. A counter-example to this is 1RXS J174537.3+395128 (Nilsson et al. 1999; Gliozzi et al. 1999) where a BLLac is found in the core of a compact lensing cluster at a redshift of 0.267. Because the ambiguity between BLLacs and central cluster galaxies is heightened at higher redshifts, future X-ray identification programmes, particularly those for the *XMM–Newton* mission whose spatial resolution may not be sufficient to resolve distant cooling flows, should be cautious when assigning identifications to radio-detected elliptical galaxies. This issue is addressed by Stocke (2001) from a perspective of misidentification of BLLacs as clusters but this study gives no clear indication that radio-loud BLLacs are being mis-identified as clusters. When it is added to the observation that many of the *ROSAT* selected BLLacs in this study have significant NVSS polarization, it may be possible to differentiate at least some of the brighter BLLacs from clusters.

7 CONCLUSIONS

We present two remarkable clusters selected from a joint radio /X-ray/optical analysis. The discovery of these clusters demonstrates that even relatively shallow X-ray surveys can uncover distant clusters if a large enough area is searched and moderately deep optical imaging can be obtained. The discoveries discussed here prompted the two lead authors to revisit the RASS and embark on a dedicated search for $z > 0.3$ clusters. Thus far, 118 X-ray luminous clusters at $z > 0.3$ have been spectroscopically confirmed, and we anticipate the total number to approach 130 on the completion of the survey (see Ebeling et al. 2001).

The radio properties of MACS J0717.5+3745 are comparable to the most powerful radio halo and relic sources known, and are consistent with the general trend for more powerful haloes in more massive clusters.

The discovery of massive distant clusters such as MACS J0717.5+3745 and MACS J1621.3+3810 provides valuable opportunities for the study of the mechanisms driving the formation and evolution of clusters and of the galaxies inhabiting them. Owing to their generic rarity, these extreme clusters are not easily found by cluster surveys at any wavelength, making the discovery of two additional systems all the more significant.

ACKNOWLEDGMENTS

We thank Pat Henry for help with some of the imaging observations discussed here and for stimulating discussions. ACE acknowledges generous support from the Royal Society. HE gratefully acknowledges financial support from NASA LTSA grant NAG 5–8253. The INT is operated on the island of La Palma by the Isaac Newton Group in the Spanish Observatorio del Roque de los Muchachos of the Instituto de Astrofisica de Canarias. We thank the University of Hawaii's Time Allocation Committee for their support of the MACS project.

This research has made use of the NASA/IPAC Extragalactic Data base (NED) which is operated by the Jet Propulsion Laboratory,

California Institute of Technology, under contract with the National Aeronautics and Space Administration. Some of the data presented here were obtained at the W. M. Keck Observatory, which is operated as a scientific partnership among the California Institute of Technology, the University of California and the National Aeronautics and Space Administration. The Observatory was made possible by the generous financial support of the W. M. Keck Foundation.

This works uses the WENSS survey funded by the Netherlands Foundation for Research in Astronomy (NFRA/ASTRON). The VLA was used extensively through the *First* and NVSS Surveys and dedicated observations so thanks go to National Radio Astronomy Observatory, a facility of the National Science Foundation operated under cooperative agreement by Associated Universities, Inc. Finally, none of this would have been possible without the existence of *ROSAT*, so our particular thanks go to the *ROSAT* team at MPE for the operation of both the survey and the pointed observations.

REFERENCES

Allen S. W. et al., 2001, MNRAS, 324, 842
Ball R., Burns J. O., Loken C., 1993, AJ, 105, 53
Bauer F. E., Condon J. J., Thuan T. X., Broderick J. J., 2000, ApJS, 129, 547
Becker R. H., White R. L., Helfand D. J., 1995, AJ, 450, 559
Böhringer H., Voges W., Fabian A. C., Edge A. C., Neumann D., 1993, MNRAS, 264, L25
Böhringer H. et al., 2000, ApJS, 129, 435
Brinkmann W., Laurent-Muehleisen S. A., Voges W., Siebert J., Becker R. H., Brotherton M. S., White R. L., Gregg M. D., 2000, A&A, 356, 445
Buote D. A., 2001, ApJ, 553, L15
Burns J. O., 1990, AJ, 99, 14
Caccianiga A., Maccacaro T., Wolter A., Della Ceca R., Gioia I. M., 2000, A&AS, 144, 247
Carilli C. L., Perley R. A., Harris D. E., 1994, MNRAS, 270, 173
Condon J. J., Cotton W. D., Greisen E. W., Yin Q. F., Perley R. A., Taylor G. B., Broderick J. J., 1998, AJ, 115, 1693
Crawford C. S., Allen S. W., Ebeling H., Edge A. C., Fabian A. C., 1999, MNRAS, 306, 857
Dickey J. M., Lockman F. J., 1990, ARA&A, 28, 215
Ebeling H., Voges W., Böhringer H., Edge A. C., Huchra J. P., Briel U. G., 1996, MNRAS, 281, 799
Ebeling H., Edge A. C., Böhringer H., Allen S. W., Crawford C. S., Fabian A. C., Voges W., Huchra J. P., 1998, MNRAS, 301, 881
Ebeling H., Edge A. C., Allen S. W., Crawford C. S., Fabian A. C., Huchra J. P., 2000, MNRAS, 318, 333
Ebeling H., Edge A. C., Henry J. P., 2001, ApJ, 553, 668
Ebeling H., Mullis C. R., Tully R. B., 2002, ApJ, 580, 774
Ebeling H., White D. A., Rangarajan V., 2003, MNRAS, submitted
Edge A. C., Stewart G. C., Fabian A. C., 1992, MNRAS, 258, 177
Ensslin T. A., Brüggen M., 2002, MNRAS, 331, 1011
Fabian A. C., Crawford C. S., 1995, MNRAS, 274, L6 10
Falco E. E. et al., 1999, PASP, 111, 438
Fischer J., Hasinger G., Schwope A., Brunner H., Boller T., Truemper J., Voges W., Neizvestny S., 1998, AN, 319, 347
Gioia I. M., Maccacaro T., Schild R. E., Wolter A., Stocke J. T., Morris S. L., Henry J. P., 1990, ApJS, 72, 567
Giovannini G., Feretti L., 2000, New Astron., 5, 335
Giovannini G., Feretti L., Venturi T., Kim K.-T., Kronberg P. P., 1993, ApJ, 406, 399
Giovannini G., Tordi M., Feretti L., 1999, NewA, 4, 141
Gliozzi M., Brinkmann W., Laurent-Muehleisen S. A., Takalo L. O., Sillanpaeae A., 1999, A&A, 352, 437
Govoni F., Feretti L., Giovannini G., Böhringer H., Reiprich T. H., Murgia M., 2001, A&A, 376, 803
Huchra J. P., Geller M. J., Corwin H. G., 1995, ApJS, 99, 391
Iwasawa K., Allen S. W, Fabian A. C., Edge A. C, Ettori S., 1999, MNRAS, 306, 467
Iwasawa K., Allen S. W., Fabian A. C., Ettori S., 2001, MNRAS, 328, L5
Kempner J. C., Sarazin C. L., 2001, ApJ, 548, 639
Laurent-Muehleisen S. A., Kollgaard R. I., Ciardullo R., Feigelson E. D., Brinkmann W., Siebert J., 1998, ApJS, 118, 127
Liang H., Hunstead R. W., Birkinshaw M., Andreani P., 2000, ApJ, 544, 686
McNamara B. R. et al., 2000, ApJ, 534, L135
Moran E. C., Helfand D. J., Becker R. H., White R. L., 1996, ApJ, 461, 127
Motch C. et al., 1998, A&AS, 132, 341
Nilsson K., Takalo L. O., Pursimo T., Sillanpaeae A., Heidt J., Wagner S. J., Laurent-Muehleisen S. A., Brinkmann W., 1999, A&A, 343, 81
Oke J. B. et al., 1995, PASP, 107, 375
Peres C. B., Fabian A. C., Edge A. C., Allen S. W., Johnstone R. M., White D. A., 1998, MNRAS, 298, 416
Perlman S., Padovani P., Giommi P., Sambruna R., Jones L. R., Tzioumis A., Reynolds J., 1998, AJ, 115, 1253
Raymond J. C., Smith B. W., 1977, ApJS, 35, 419
Rengelink R. B., Tang Y., de Bruyn A. G., Miley G. K., Bremer M. N., Röttgering H. J. A., Bremer M. A. R., 1997, A&AS, 124, 259
Röettiger K., Loken C., Burns J. O., 1997, ApJS, 109, 307
Röettiger K., Burns J. O., Stone J. M., 1999, ApJ, 518, 603
Röttgering H. J. A., Snellen I., Miley G., de Jong J. P., Hanisch R. J., Perley R., 1994, ApJ, 436, 654
Röttgering H. J. A., Wieringa M. H., Hunstead R. W., Ekers R. D., 1997, MNRAS, 290, 577
Schwope A. et al., 2000, AN, 321, 1
Stocke J. T., 2001, in Padovani P., Urry C. M., eds, ASP Conf. Ser. Vol. 227, Blazar Demographics. Astron. Soc. Pac., San Francisco, p. 184
Tribble P. C., 1993, MNRAS, 263, 31
Vikhlinin A., McNamara B. R., Forman W., Jones C., Quintana H., Hornstrup A., 1998, ApJ, 502, 558
Voges W. et al., 1999, A&A, 349, 389
Wei J. Y., Xu D. W., Cao L., Zhao Y. H., Hu J. Y., Li Q. B., 1998, A&A, 329, 511
Wei J. Y., Xu D. W., Dong X. Y., Hu J. Y., 1999, A&AS, 139, 575
White D. A., Jones C., Forman W. R., 1997, MNRAS, 292, 419

This paper has been typeset from a TEX/LATEX file prepared by the author.